

Exploring Hemodynamics by Raycasting 4D MRI Flow

R. van Pelt¹, J. Oliván Bescós², M. Breeuwer², M. E. Gröller³, B. ter Haar Romeny¹ and A. Vilanova¹

¹Department of Biomedical Engineering, Eindhoven University of Technology, The Netherlands

²Department of Clinical Sciences and Advanced Development, Philips Healthcare, The Netherlands

³Department of Computer Graphics and Algorithms, Vienna University of Technology, Austria

Keywords: Volume Visualization, Flow Visualization, Raycasting, Magnetic Resonance Angiography.

Abstract

Flow sensitive phase-contrast magnetic resonance imaging sequences produce three-dimensional velocity fields in time, providing quantitative information of blood flow dynamics. Thorough understanding of the hemodynamic behavior will support physicians to diagnose and assess risk of various cardiovascular diseases. However, inspection of the complex cine flow data, encompassing both morphology and function, is generally a troublesome and tedious task. Over the last few decades, the field of scientific flow visualization has introduced a multitude of techniques to explore unsteady velocity fields, in order to capture and depict flow characteristics. Inspired by concepts from ultrasound imaging, we have investigated raycasting as a means to explore and visualize direction and magnitude of blood velocities, striving to reveal the blood flow behavior. In particular, we aim to depict flow patterns that deviate from the expected blood flow. For that purpose, several interaction techniques have been incorporated into the presented framework. Angles between a user-defined direction, set by an interaction widget, and the velocity field are mapped to different visual cues using a transfer function. Furthermore, we define the prevalent flow as approximate of the expected blood flow, generated based on the vessel centerline. We visualize a projection of the angles between the prevalent flow and the velocity field.

1 Introduction

Magnetic Resonance Imaging (MRI) techniques are known to acquire accurate anatomic depictions of the heart and vessels. In addition, the MRI acquisition process is intrinsically sensitive to flow. Phase-Contrast (PC) MRI sequences exploit this characteristic to obtain quantitative information of the blood flow within a predefined velocity range. Typical PC protocols provide a two-dimensional slab, comprising the through-plane flow directions. Best results are

achieved when the slab is acquired orthogonal to the vessel structure of interest, requiring careful planning by a skilled operator.

Three-dimensional, isotropic PC-MRI imaging sequences overcome the operator dependency, and rule out repeated acquisitions when the resulting quality does not meet expectations. The desired slab can be determined offline, by a planar reformat of the volumetric data. Generally, the data is inspected based on the reformatted slab, using both qualitative and quantitative techniques similar to the ones applied for two-dimensional PC imaging.

Current research concerning cardiac and vascular flow behavior focusses on understanding flow patterns. Various publications describe strong indications that atypical flow patterns can be related to medical conditions [1, 4, 5, 11]. Therefore, insight into the hemodynamics is necessary to reveal these relations. In the future, knowledge of the hemodynamics might support diagnosis and risk assessment of various cardiovascular diseases. Important application areas can be found in congenital diseases, valvular diseases and aortic anomalies.

There is strong interest in quantitative information derived from the blood flow velocity field. This information enables objective assessment of the blood flow, based on a wide range of parameters. By means of these derived parameters, interpatient and inpatient comparisons can be performed to analyze variations of the hemodynamics.

Furthermore, blood flow information potentially reveals characteristics of anatomical structures that are hardly visible on typical morphologic acquisitions. Small structures, such as the valves or the septum, are too small to image with most acquisition protocols. However, the surrounding velocity field can provide valuable information about the condition of the structure of interest.

Insight into the complex behavior of unsteady blood flow can be obtained by means of expressive visualization and intuitive interaction. However, visualization of three-dimensional unsteady flow fields

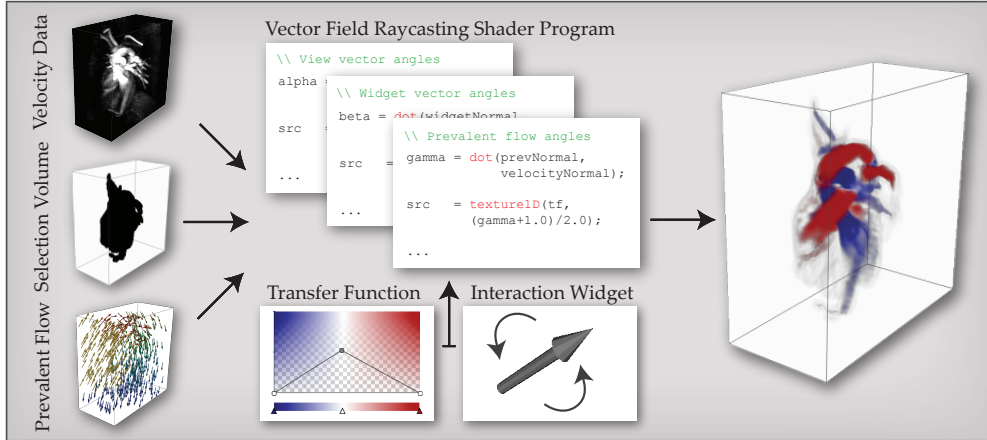


Figure 1: Overview of the presented framework: vector field raycasting by angle composition. The 4D velocity field is available to the shader program, together with the segmentation and prevalent flow volumes. The shader program traverses the user-defined angles and depicts the resulting composition

is challenging. The multidimensional data has to be mapped to lower dimensional visual cues, and visual clutter should be avoided.

A common visualization technique is the multi-planar reformat (MPR), extracting an oblique slice from the volume data. For vector fields, the MPR is typically color coded by means of the through-plane and in-plane components of the velocity field vectors. An MPR provides a straight-forward approach to reduce dimensionality, which has the drawback to neglect a vast amount of relevant information. More elaborate methods that are commonly applied include glyphs, particle traces, streamlines and pathlines. These concepts require elaborate and time-consuming parametrization to produce meaningful results.

In this paper, we explore new approaches to convey both direction and magnitude of the complex velocity field. We were inspired by ultrasound blood flow imaging, where flow is encoded relative to the imaging probe. The colors blue and red encode the flow direction, respectively away from and towards, the probe. Most medical practitioners are familiar with this two-dimensional concept, and therefore we have elaborated on this approach, using interactive direct volume rendering on the time-resolved blood flow data.

The direct volume rendering approach is based on raycasting, producing a holistic view of features in a volumetric data sets. A transfer function provides a flexible tool to interactively map data characteristics to visual cues. Our GPU-based method is based on the projection of angles between a user-defined direction and the velocity field.

The presented framework includes different ways to interactively explore the data. Furthermore, we assess different approaches to depict direction and mag-

nitude of the velocity field, mapping these data characteristics to color and opacity.

In summary, the main contributions of this paper are:

- Visualization of direction and magnitude of complex 4D unsteady blood flow MRI data, using vector field raycasting by angle composition. (section 4)
- Different user interaction approaches to explore the blood flow velocity field. (section 4)
- Visual assessment of the mapping of data characteristics to visual cues. (sections 5 and 6)

In the following, we first present the related work. After a short overview of the MRI acquisition configuration, we elaborate on the vector field raycasting approach, based on angle composition. Several interaction methods are presented, after a description of the required pre-processing steps. Subsequently, we show several mappings of the angle composition to visual cues. Lastly, we discuss the results, followed by our conclusions and suggestions for future work.

2 Related work

2.1 Blood Flow Imaging

There is a growing interest to study hemodynamics based on time-resolved in vivo MRI. Different MRI protocols enable acquisition of blood flow information. We focus on PC-MRI related publications for cardiovascular applications.

Many studies investigate flow patterns in congenital heart disease patients. Blood flow patterns can be heavily disturbed, and proper understanding of the hemodynamics is valuable for both planning and

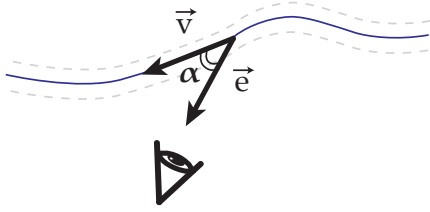


Figure 2: Vector field raycasting by composing angles α between the view direction \vec{e} and the blood flow velocities \vec{v} .

follow-up. For example, Sørensen et al. [11], presented a significant study, investigating 4D PC-MRI for congenital heart diseases, using a combination of existing visualization techniques.

Furthermore, the aorta is a cardiovascular structure of interest with respect to its blood flow behavior. In this paper we focus on the hemodynamics in the upper aorta. There is active research aiming to understand the flow behavior in both the upper and abdominal aorta, even in the case of healthy volunteers. For instance, Bogren et al. [1] studied the helical flow in the aorta, for healthy young and elderly volunteers. Furthermore, flow behavior surrounding aortic anomalies is of great interest. A particular study concentrating on aortic aneurysms is presented by Hope et al. [5], while Harloff et al. had their focus on the detection of plaques in the descending aorta [4].

Apart from the cardiovascular applications, there is also a vast interest for blood flow behavior in the cranium. Similarly, there is still lack of understanding of the complex blood flow in the human neurovascular system. Therefore, research focusses on both visualization techniques, such as presented by Yamashita et al. [10], and quantitative measurements, like the work presented by Wetzel et al. [13].

2.2 Flow and Volume Visualization

In scientific visualization, flow visualization has been a prominent field of interest in the last few decades. The field can be roughly divided into two areas, which both have been comprehensively described in a profound state-of-art report. The first area considers dense texture based visualization methods, which are typically effective for 2D visualization purposes. Advancements in this area were described by Laramee et al [6]. The second area focusses on feature-based visualization based on the vector field topology, which was distinctly described by Post et al. [8]. Recent work on multi-dimensional vector field topology is presented by Weinkauff [12], and feature extraction in time-dependent flow data is extensively studied by Fuchs [3].

Typical visualization techniques, used by re-

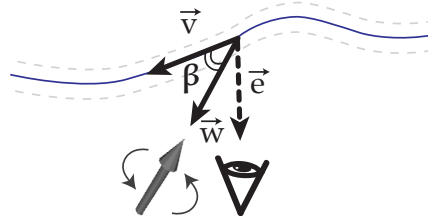


Figure 3: Vector field raycasting by composing angles β between widget direction \vec{w} and the blood flow velocities \vec{v} .

searchers in the medical domain, capture the structure in the spatial domain by means of stream objects, such as stream lines or stream tubes. Less common is the glyph based approach, typically depicting the velocity field structure at one moment in time by two or three-dimensional arrows. The structure in the temporal domain is typically conveyed by means of particle traces, or pathlines. Many of these approaches are combined with an MPR or a direct volume rendering to add anatomical context (e.g., Sørensen et al. [11]).

All of these approaches, with the exception of the glyph based method, require a precise definition of a seeding region. Visual results heavily depend on user-defined parameters, which mostly can not be adapted interactively. We have investigated a direct volume rendering approach, comparable to the work presented by Frühauf [2]. He proposed a method to raycast vector fields, incorporating shading and pseudo-colors. For our purpose, shading is not an intuitive visual cue. However, we perform raycasting on the 4D velocity field by means of an angle composition, as described in section 4. The GPU-based raycasting approach relies on the work presented by Scharsach [9].

3 Phase-Contrast MRI

The 4D blood flow velocity data is acquired by a PC-MRI sequence, using a Philips Achieva MR scanner at a field strength of 3 Tesla. A full cardiac cycle is retrospectively reconstructed in 25 phases, using both cardiac and respiratory gating. Each phase consists of a 3D velocity vector field, with quantitatively defined directions and magnitudes. The data for each phase has a resolution of $128 \times 128 \times 52$ voxels, with a voxel size of $2.1\text{mm} \times 2.1\text{mm} \times 2.5\text{mm}$. The approach was verified on three similar data sets of healthy volunteers.

4 Vector Field Raycasting by Angle Composition

A global overview of the GPU-based vector field raycasting framework is depicted in figure 1. This

section describes the framework, comprising different approaches to raycast the blood flow velocity field.

4.1 Pre-processing

The velocity-encoded data typically contains a considerable amount of acquisition artefacts, in particular in the stationary areas. Incorrect high intensity values in these areas lead to erroneous velocity vectors. For that reason, the structures of interest need to be segmented, removing these erroneous vectors. In the past, extensive automated segmentation methods have been presented, such as the level set approach by Persson et al. [7]. We focus on the visualization aspects, and take a manual approach to segment the structures. This allows us to define, select and visualize the desired structures.

Manual segmentation of all cardiac phases for each of the data sets is a tedious task, while an exact segmentation of the structures for each phase is not strictly required. Instead, a static segmentation of the areas where flow can occur suffices to suppress the erroneous velocity vectors in regions without blood flow. This oversized segmentation can be applied to all phases of the cardiac cycles, and by definition encompasses the blood flow volume-of-interest.

For this purpose, a new volumetric data set is derived from the full cine velocity data ($v_i(\vec{x})$). For each voxel position \vec{x} of the new volume, the maximum velocity magnitude is projected along the time axis t . This process, called a Temporal Maximum Intensity Projection (T-MIP), is defined as follows for T cardiac phases:

$$\text{T-MIP}(\vec{x}) = \max_i (\|v_i(\vec{x})\|) \quad \text{for } i = 0, \dots, T - 1$$

The T-MIP volume encodes all areas where flow occurs in one of the cardiac phases by high intensities, taking the pulsating movement of the aorta into account. Note that also the erroneous velocity vectors may be projected into the new volume. Therefore a manual segmentation is required, for which the T-MIP volume provides a proper basis. This reduces the manual workload to only a single volume, as opposed to a volume for each of the cardiac phases.

The resulting segmentation is stored as a binary selection volume, and is provided to the shader program (see figure 1). In this paper, we focus on the upper aorta. In all figures throughout the paper, the segmented area is depicted by a semi-transparent surface, providing context to the blood flow features. Keep in mind that this surface represents the largest volume in which flow can occur over time, as opposed to the morphological boundary of the vessel structure.

4.2 Angles: User-Defined Vector and Velocity Field

Using the vector field raycasting approach, we strive to reveal both directions and magnitudes of the unsteady flow field. Straightforward color-mappings do not suffice, since vectors of the velocity field have a sign. We propose an approach to raycast the multi-dimensional vector field, compositing angles between a user-defined vector and the velocity field vectors. This allows directions and magnitudes to be conveyed using limited visual cues, while interactively exploring the data.

In the first approach, schematically depicted in figure 2, the raycasting is based on the angles between the view direction \vec{e} and the velocity field vectors $\vec{v}(\vec{x})$. The solid blue line depicts the direction of the velocity field, where only vector \vec{v} is highlighted. The dashed lines illustrate the continuation of velocity field, outside the scope of the considered vector. In the remainder of this chapter, all operations take place in the spatial domain, and therefore time will be discarded in the formulations. For each position \vec{x} in the volume, the angle is determined by the dot product as follows:

$$\alpha(\vec{x}) = \arccos(\vec{e} \cdot \vec{v}(\vec{x}))$$

In case the directions of vectors \vec{e} and $\vec{v}(\vec{x})$ are equal, hence an angle of 0° , the flow direction is moving *towards* the viewer. We adhere to the 2D ultrasound convention, and generally encode this with the color red. Similarly, opposite vectors with an angle of 180° , are encoded with the color blue. This is schematically depicted in figure 4, where a diverging color map is applied. Saturation decreases when moving from parallel to orthogonal vector orientations. Note the symmetric angles with the view vector cannot be distinguished. The proposed color-coding is merely a convention, and can be easily changed by means of the interactive transfer-function editor.

Using the view vector to define the angles in the raycasting approach, implies a view-dependent color mapping. Rotating the data set, together with ani-

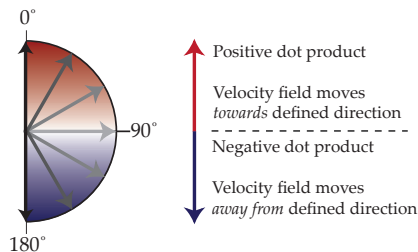


Figure 4: Color coding of the angles between a user-defined vector and the velocity field vectors, inspired by the ultrasound convention. Angles are determined by the dot product.

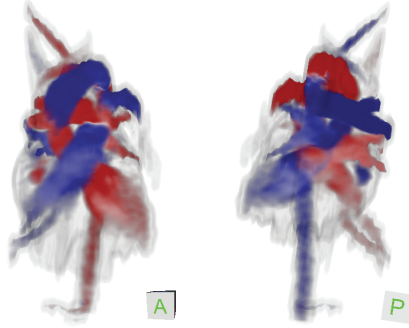


Figure 5: Color and/or opacity composition is view-dependent, when inspecting the velocity field with the view vector. Colors invert when opposite view directions are chosen. (A = Anterior; P = Posterior)

mation over time, gives an intuition of the direction of the flow at a particular time in the cardiac cycle. While exploring the data, the color-coding convention of blood flowing away and towards the viewer remains. Figure 5 clearly shows this view dependency, by taking opposite views on the velocity field. For example, in the anterior view the flow in the upper arch of the aorta is colored blue, hence moving away from the viewer. However, in the posterior view the flow in the upper arch of the aorta is colored red, and thus expectedly moves towards the viewer.

Alternative to the view-vector approach, the interaction widget, depicted in figure 1, provides a more generic way to set the angles for compositing. This widget represents a fixed direction \vec{w} , from which the angles $\beta(\vec{x})$ along the ray are determined as:

$$\beta(\vec{x}) = \arccos(\vec{w} \cdot \vec{v}(\vec{x}))$$

Figure 3 schematically depicts the approach, using the interaction widget to explore the data. The view-vector dependent angle-selection method can be considered as a special case of the interaction-widget approach. However, the latter is not view-dependent. Therefore, the result of a chosen direction \vec{w} can be inspected from any viewpoint. The user is able to set

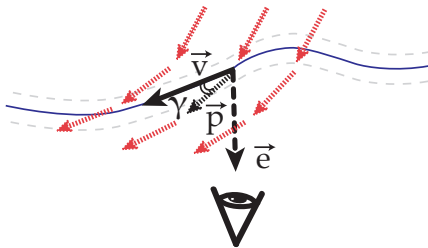


Figure 6: Vector field raycasting by compositing the angles γ between the prevalent flow direction \vec{p} and the blood flow velocities \vec{v} . The dotted arrows depict the prevalent flow.

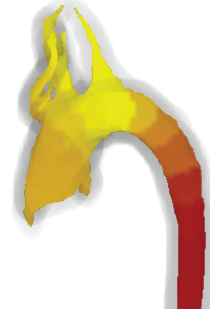


Figure 7: The prevalent flow is the expected flow, in the direction along the centerline of the aorta. The x -component of the vectors are color-coded, and depicted with the surface of the manual segmentation.

the widget direction parallel or orthogonal to the expected direction of the flow field in a particular structure of interest.

4.3 Angles: Prevalent Flow and Velocity Field

The previous subsection introduced the notion of vector field raycasting based on angle composition, emphasizing the direction of the blood flow. However, general directions of the flow within the cardiovascular structures are defined by the function of the heart. Instead of inspecting merely the direction of blood flow, it is relevant to depict deviations from the expected flow. This is generally a time-consuming task with currently existing techniques.

For this purpose, a volume is generated, encompassing a normalized vector field in the expected direction of the blood flow. This volume is called the *prevalent flow* and is provided to the shader program, as depicted in figure 1. Subsequently, the angles between the prevalent flow directions $\vec{p}(\vec{x})$ and the velocity field vectors $\vec{v}(\vec{x})$ can be composited along the ray positions \vec{x} , as follows:

$$\gamma(\vec{x}) = \arccos(\vec{p}(\vec{x}) \cdot \vec{v}(\vec{x}))$$

Figure 6 schematically depicts the approach, where the dashed diagonal arrows portray the prevalent flow directions, and where \vec{p} represents the particular flow direction under consideration. Observe that the resulting visualization using this approach requires different interpretation. Small angles indicate that the velocity field vector properly follows the expected flow direction. More interestingly, obtuse vectors indicate regurgitant flow with respect to the prevalent flow.

For the presented figures in this paper, and as a proof of concept, the prevalent flow field is generated based on the centerline of the upper aorta. For each voxel in the prevalent flow volume, the nearest

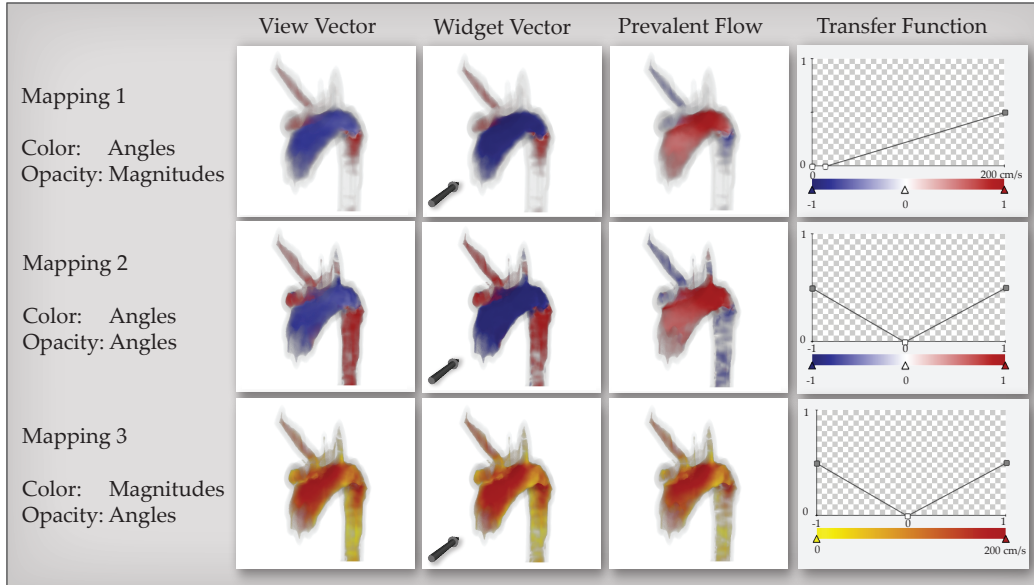


Figure 8: Presented methods to determine the angles for vector field raycasting, with various mappings to visual cues. Angles are defined by the dot product, within the range $[-1,1]$. Magnitudes are defined by the maximum speed, within the range $[0 \text{ cm/s}, 200 \text{ cm/s}]$.

point on the centerline is determined, and the direction along the centerline is adopted to generate the vector field. Figure 7 shows a color-coding of the x -component of the prevalent flow directions, depicted together with the segmentation surface as context. The prevalent flow clearly follows the centerline of the aorta.

Section 6 describes additional results of the presented vector field raycasting approach. However, the different ways to map the data characteristics to visual cues will be elaborated in section 5 first.

5 Mapping Visual Cues

The vector field raycasting approaches incorporate an angle composition by which directionality can be mapped to a visual cue. Additionally, the quantitative speed of the velocity field is a relevant characteristic that should be conveyed in the resulting visualization.

The primary visual cues for direct volume rendering are color and opacity. The notion of shading, as presented for vector fields by Frühauf et al. [2], is deliberately not incorporated into the framework. Applying diffuse shading highlights areas near the light source, and suppresses areas further away from the light source. This generally provides a better perception of depth on the blood flow features, but the lighting accents are easily interpreted as a variation of speed of the blood flow.

Figure 8 presents an overview of the various raycasting approaches, differently mapped to color and opacity. Since direction of the velocity field is the primary characteristic, we have excluded the mapping of

velocity magnitudes to both color and opacity.

Observe that the color lookup table and opacity function should be adapted to the corresponding characteristic. First, we consider the color lookup table. In case directionality is mapped, using the angles computed along the ray, a diverging color map provides most intuitive results. This way, parallel vectors are visually distinguished, and saturation is reduced when moving toward orthogonally oriented vectors. In subsection 4.2, we proposed the red and blue color coding, based on the ultrasound convention. Alternatively, when magnitudes are mapped to color (mapping 3), a linear gradient is more suitable.

Next, we consider the opacity function. In case the directionality of the velocity field is mapped to opacity, again the parallel vector orientation should be emphasized. This can be accomplished by a 'v'-shaped function. When velocity magnitudes are mapped onto the opacity (mapping 1), a linear function emphasizes the areas where the blood flows fast. Typically, a small interval of the range of smallest magnitudes is suppressed, to avoid noise patterns between the vessel wall and the segmentation.

Alternative parameterizations of the transfer function can easily be investigated. For instance, one may stress the areas where the blood flows perpendicular to the user-defined vector, instead of emphasizing parallel orientations.

Applying different mappings enables exploration of the data by highlighting different data characteristics. Directionality is in this case the most relevant characteristic, and is conveyed best by a color mapping. Directionality can be mapped to both color and

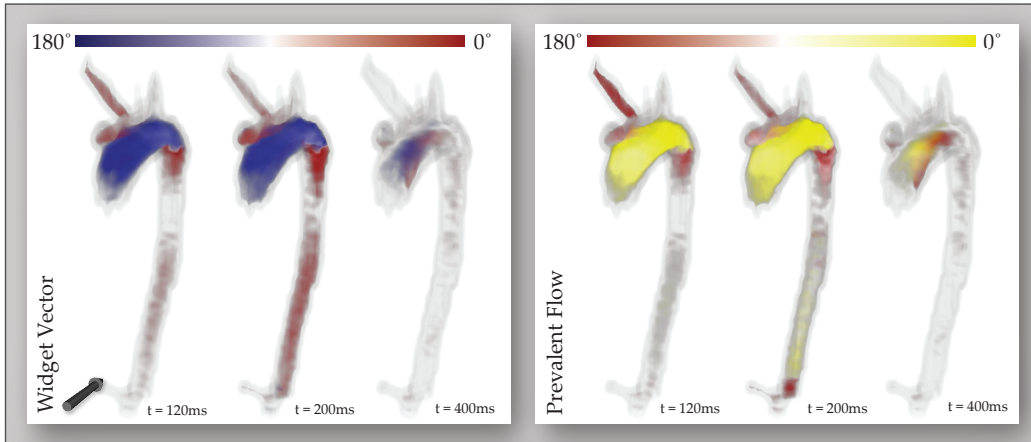


Figure 9: Results with the angle composition mapped to color, and velocity magnitudes mapped to opacity. *Left*: angles determined by the widget vector. Encodes blue blood flowing away from the widget direction; red encodes blood flowing towards the widget direction. *Right*: angles determined by the prevalent flow volume. Yellow encodes perfect alignment of the flow directions with the prevalent flow, while red encodes flow against the expected prevalent directions.

opacity, discarding magnitude information. However, this magnitude information enables to select only the areas where the blood flow is pronounced. This is generally conveyed best by a mapping to opacity.

6 Results

The results in figure 8 for the view-vector and widget-vector raycasting approach show strong similarities. The widget-vector is oriented maximally parallel to the velocity field vectors, which in this case nearly corresponds to the view-direction. The widget vectors shows directionality slightly more pronounced. The results, which strongly depend on interactive inspection and time animation, should be interpreted as described in subsection 4.2.

A different interpretation of the visualization results is required when using the prevalent flow to determine the angles for composition (see figure 8). Using the same color lookup table, red encodes the areas where the velocity field vector follows the prevalent flow to a large extent. Blue encodes the other extremity, where the velocity field vectors are directed against the expected flow direction. Be aware that with the second and third mapping noise is not suppressed by setting the lowest magnitudes fully transparent. This introduces some artefacts near the vessel wall, where noise is included in the ray compositing.

Figure 9 shows the results for both the widget-vector approach and the prevalent flow based approach. Considering the ad hoc findings described in section 5, mapping 1 is applied. Hence, color encodes the directions of the velocity field, while opacity encodes the speed. For each method, three phases of the cardiac cycle are presented. The first two phases are

part of the systole phase of the cardiac cycle, where the heart pumps blood into the aorta. The third phase is part of the diastole phase of the cardiac cycle, where the heart relaxes and is filled with blood.

On the left, the widget-vector approach shows that blood flows away from the widget-vector in the upper arch of the aorta. Subsequently, the blood flow makes a coarse helical movement towards the abdominal aorta. This can be seen from the red encoding, indicating the flow direction is now opposite to the widget-vector. The first two phases show a clear blood filling of the aorta, while in the last phases the flow is dropped.

On the right, the prevalent flow is encoded with a different color map, where blood flow along the prevalent flow direction is yellow and opposite flow is encoded with red. Similar to the widget-vector approach, we see a filling of the aorta in the first two cycles. Additionally, an area with turbulent behavior of the flow can be observed at the second presented phase, right after the upper arch. Moreover, we see that during the diastole phase some flow moves backwards in the direction of the valve. This can be derived from the red encoded region in the third presented phase.

7 Conclusions

In the previous, we have presented experiments with a direct volume rendering approach to explore 4D PC-MRI blood flow, focussing on the upper aorta. We have introduced a vector field raycasting by means of angle composition, which can be interactively parameterized by different mappings to visual cues. Color and opacity mapping can be changed fast and

intuitively by means of a transfer function. This in contrast to generally complicated, non real-time parameterization of other customary techniques, such as streamlines and particle traces. Our framework requires only limited pre-processing steps.

The initial results successfully show that direction and magnitude of the complex unsteady blood flow can be conveyed, while exploring the data by means of interaction and animation. We rely on MRI acquired data, which makes the approach more dependable than Computational Fluid Dynamics (CFD) simulations, which are based on a considerable amount of model assumptions.

The current framework still imposes some limitations. Typically, the angle composition accumulates quickly to opaque, fully saturated colors. Therefore, subtle details of variation in the flow are lost. Also the prevalent flow approach, which provides a way to visualize flow areas that deviate from the expected flow directions, can be improved. The prevalent flow field currently follows the centerline of the aorta, and does not take helical flow into account.

8 Future Work

At this point, the framework is capable to depict the global characteristics of the complex PC-MRI data. With the prevalent flow approach, we show that visualization of the deviations of the expected flow is indeed promising. Especially in combination with interactive exploration methods, such as the view-vector and widget-vector based approach.

The framework can be improved by introducing a more accurate prevalent flow field, resulting in enhanced depictions of deviating flow patterns. One could think of an artificial flow field, incorporating the expected helicity of the flow, or even a field generated by CFD simulations. This is a challenging subject, since the direction of the helical flow varies from person to person. This direction should therefore be automatically determined a priori.

The presented vector field raycasting technique should be assessed by experts in the application domain. We believe that with this method, deviating patterns, such as phase wraps, regurgitations and vortices, can be easily detected.

In the future, patient data will provide new visualization challenges. Specific cases of cardiovascular diseases require different visualization techniques. Also then, proper validation of the results in the medical domain is necessary.

References

- [1] H. G. Bogren and M. H. Buonocore. 4d magnetic resonance velocity mapping of blood flow patterns in the aorta in young vs. elderly normal subjects. *Magnetic Resonance Imaging*, 10(5):861–869, 1999.
- [2] T. Fruhauf. Raycasting vector fields. In *Proceedings of IEEE Visualization '96*, pages 115–ff., Los Alamitos, CA, USA, 1996.
- [3] R. Fuchs. *The Visible Vortex - Interactive Analysis and Extraction of Vortices in Large Time-Dependent Flow Data Sets*. PhD thesis, Institute of Computer Graphics and Algorithms, Vienna University of Technology, Oct. 2008.
- [4] A. Harloff, C. Strecker, and A. P. Frydrychowicz. Plaques in the descending aorta: A new risk factor for stroke? visualization of potential embolization pathways by 4d mri. *Magnetic Resonance Imaging*, 26 6:1651–1655, 2007.
- [5] T. A. Hope, M. Markl, L. Wigström, M. T. Alley, D. C. Miller, and R. J. Herfkens. Comparison of flow patterns in ascending aortic aneurysms and volunteers using four-dimensional magnetic resonance velocity mapping. *Magnetic Resonance Imaging*, 26:1417–1479, 2007.
- [6] R. S. Laramée, H. Hauser, H. Doleisch, B. Vrolijk, F. H. Post, and D. Weiskopf. The state of the art in flow visualization: Dense and texture-based techniques. *Computer Graphics Forum*, 23:2004, 2004.
- [7] M. Persson, J. E. Solem, K. Markenroth, J. Svensson, and A. Heyden. Phase contrast mri segmentation using velocity and intensity. *Scale Space and PDE Methods in Computer Vision*, pages 119–130, 2005.
- [8] F. H. Post, B. Vrolijk, H. Hauser, R. S. Laramée, and H. Doleisch. The state of the art in flow visualisation: Feature extraction and tracking. *Computer Graphics Forum*.
- [9] H. Scharsach. Advanced gpu raycasting. In *Proceedings of CESC*, 2005.
- [10] M. H. Shuhei Yamashita, Haruo Isoda. Visualization of hemodynamics in intracranial arteries using time-resolved three-dimensional phase-contrast mri. 25 3:473–478, 2007.
- [11] T. S. Sørensen, P. Beerbaum, H. Körperich, and E. M. Pedersen. Three-dimensional, isotropic mri: a unified approach to quantification and visualization in congenital heart disease. *The International Journal of Cardiovascular Imaging*, 21(2):283–292, Apr 2005.
- [12] T. Weinkauff. *Extraction of Topological Structures in 2D and 3D Vector Fields*. PhD thesis, University Magdeburg, 2008.
- [13] S. Wetzel, S. Meckel, A. Frydrychowicz, L. Bonati, E.-W. Radü, K. Scheffler, J. Hennig, and M. Markl. In vivo assessment and visualization of intracranial arterial hemodynamics with flow-sensitized 4d mr imaging at 3t. *Neuroradiology*, 28(3):433–438, 2007.